

# Effect of Neodymium Doping on MRI Relaxivity of Gadolinium Oxide Nanoparticles

Divband B.<sup>1,2,3</sup>, Gharehaghaji N.<sup>4\*</sup>, Takhiri M.<sup>5,6</sup>

## ABSTRACT

**Background:** Gadolinium oxide nanoparticles as positive contrast material of magnetic resonance imaging (MRI) have attracted a great attention due to the appropriate magnetic properties. One of the most desirable features of these nanoparticles is their ability of doping with other lanthanides which can change their properties.

**Objective:** This study aimed to investigate the effect of neodymium doping on MRI relaxivity of the gadolinium oxide nanoparticles.

**Material and Methods:** In this experimental study, the oleic acid coated gadolinium oxide nanoparticles and the neodymium doped nanoparticles were prepared by polymer pyrolysis method. X-ray diffraction test and scanning electron microscopy were used for characterization of the particles. 3-(4,5-dimethylthiazol-2-yl)-2,5-diphenyltetrazolium bromide (MTT) assay was performed to investigate the in vitro cell toxicity of the nanoparticles. The r1 and r2 relaxivities were extracted from the T1 and T2 weighted MR images, respectively.

**Results:** The average size of the cytocompatible spherical-like shape nanoparticles was 40 nm. The neodymium doped nanoparticles produced a significant decrease in the r1 relaxivity, and a 1.7 fold increase in the r2 relaxivity compared to the gadolinium oxide nanoparticles.

**Conclusion:** Doping of neodymium into the gadolinium oxide nanoparticles suppresses the r1 relaxivity and enhances the r2 relaxivity of the nanoparticles.

**Citation:** Gharehaghaji N, Divband B, Takhiri M. Effect of Neodymium Doping on MRI Relaxivity of Gadolinium Oxide Nanoparticles. *J Biomed Phys Eng.* 2020;10(5):589-596. doi: 10.31661/jbpe.v0i0.2008-1165.

## Keywords

Relaxivity; Magnetic Resonance Imaging; Doping; Gadolinium Oxide; Nanoparticles; Neodymium

## Introduction

Magnetic resonance imaging (MRI) has an important role in diagnosis of different diseases involving body soft tissues [1]. To obtain better diagnosis and differentiation of the lesions, using of MRI contrast media is essential in many cases [2, 3]. Contrast agents in MRI influence image contrast by changing longitudinal (T1) and transverse (T2) relaxation times of the protons. Gadolinium (Gd<sup>3+</sup>) based contrast materials are positive contrast agents due to their obvious impact on longitudinal relaxation time of water protons [2]. Gadolinium is a choice positive contrast agent in MRI because of the seven unpaired electrons which make it one of the elements with a high magnetic moment [4]. In addition, gadolinium based nanomaterials have potential

<sup>1</sup>PhD, Medical Radiation Sciences Research Team, Tabriz University of Medical Sciences, Tabriz, Iran

<sup>2</sup>PhD, Dental and Periodontal Research Center, Tabriz University of Medical Sciences, Tabriz, Iran

<sup>3</sup>PhD, Inorganic Chemistry Department, Chemistry Faculty, University of Tabriz, C.P. 51664 Tabriz, Iran

<sup>4</sup>PhD, Department of Radiology, Faculty of Paramedicine, Tabriz University of Medical Sciences, Tabriz, Iran

<sup>5</sup>MSc, Department of Radiology, Faculty of Paramedicine, Tabriz University of Medical Sciences, Tabriz, Iran

<sup>6</sup>MSc, Medical Imaging Center, Emam Reza Hospital, Iranian Social Security Organization, Urmia, Iran

\*Corresponding author: N. Gharehaghaji  
Department of Radiology, Faculty of Paramedicine, Tabriz University of Medical Sciences, Tabriz, Iran  
E-mail: gharehaghajin@tbzmed.ac.ir

Received: 22 August 2020  
Accepted: 14 September 2020

for anticancer drug loading and tumor targeting [5, 6]. Size, shape and surface properties of gadolinium based nanomaterials are the important factors that influence correlation of gadolinium ions with water protons [7]. Unlike positive contrast media of MRI, negative contrast enhanced materials show a higher effect on transverse relaxation rate of water protons [8].

Recently, gadolinium oxide nanoparticles ( $Gd_2O_3$ ) have been developed as a high-performance positive contrast material for MR imaging [9, 10]. Due to the high surface-to-volume ratio of  $Gd_2O_3$  nanoparticles, their effect on longitudinal relaxation rate of the protons is higher than that of gadolinium chelates [11].  $Gd_2O_3$  nanoparticles can be doped into the other lanthanides. In doping process, some impurities of the lanthanide is added to  $Gd_2O_3$  nanoparticles, leading to changes in the nanoparticles properties [12]. Since some of the lanthanides such as  $Tb^{3+}$  and  $Eu^{3+}$  have optical properties, by introducing these elements into  $Gd_2O_3$  nanoparticles, optical properties are added to the nanomaterials. Therefore, the terbium doped  $Gd_2O_3$  nanoparticles [13], and the europium doped nanoparticles [14, 15] have been investigated for dual mode MRI/fluorescence imaging in other studies. In addition to applications of doped  $Gd_2O_3$  nanoparticles in the imaging methods, the rare earth or lanthanide doped  $Gd_2O_3$  nanoparticles along with other materials have been studied for other biomedical applications such as drug delivery [16, 17], tumor targeting [18], and photodynamic therapy [19, 20].

Neodymium (Nd) is one of the rare elements. The optical properties of the neodymium doped  $Gd_2O_3$  nanorods have been investigated [21]. However, to the best of our knowledge, the effect of neodymium doping into  $Gd_2O_3$  nanoparticles ( $Nd^{3+}:Gd_2O_3$ ) on the MRI r1 and r2 relaxivities of the particles has been not considered. Therefore, the purpose of the current study was to investigate the effect of  $Nd^{3+}$  doping on MRI relaxivity of the gado-

linium oxide nanoparticles.

## Material and Methods

### Preparation of the oleic acid coated $Nd^{3+}:Gd_2O_3$ nanoparticles

In this experimental study, preparation of the  $Gd_2O_3$  nanoparticles was carried out based on Katamian et al., study [22]. For this purpose, 0.9 mmol  $GdCl_3 \cdot 6H_2O$  was dissolved in 2 ml dilute nitric acid ( $2 \text{ mol L}^{-1}$ ) and 2.7 mmol citric acid was added to the solution. The mixture was stirred during 3 h. By using dilute ammonia, the final pH was controlled to be 6-7 (Solution A). As the next step, the acrylamide monomers (0.5 g) were added into the clear solution A and was stirred for 20 min (Solution B). Then, the resulted solution was heated in a water bath. The system was stirred continuously during the whole process. As the temperature was increased, the solution was became gradually transparent. For the synthesis of  $Nd^{3+}:Gd_2O_3$  nanoparticles, the proper amount of  $Nd_2O_3$  added into the transparent solution of Nd:Gd was 3:100. At the temperature about  $80 \text{ }^\circ\text{C}$ , a little amount of compound initiator AIBN ( $C_8H_{12}N_4$ ) was added into the solution which led to a quick polymerization. Subsequently, the transparent polymeric resin was obtained with no precipitation. At the last step, to achieve a xerogel, the synthesized gel was dried at  $100 \text{ }^\circ\text{C}$  for 24 h. Then, in order to burn out the organic residues, the xerogel was heated at  $300 \text{ }^\circ\text{C}$  in a laboratory furnace for 10 h and calcined at  $550 \text{ }^\circ\text{C}$  for 5 h.

For preparation of the oleic acid coated  $Nd^{3+}:Gd_2O_3$  nanoparticles [11], 100 mmol oleic acid was added to 1 mL of  $Nd^{3+}:Gd_2O_3$  nanoparticles suspension which was dispersed in ethyl ether 3000 mg/L of  $Gd^{3+}$  concentration. After 24 h stirring, sodium bicarbonate solution (0.1 M) with a pH of 9 was added and stirring was performed for 2 h. Then, for dispersion of oleic acid coated  $Gd_2O_3$  in water, a probe solicitor with amplitude of 60% was used for 10 minutes. In order to complete

evaporation of ethyl ether, the suspension was stirred for 1 day at room temperature. For purification of the oleic acid coated Nd<sup>3+</sup>:Gd<sub>2</sub>O<sub>3</sub> nanoparticles, syringe filtration with 90 °K was used.

### Characterization

The crystal structure of the nanoparticles was detected by powder X-ray diffraction (XRD) using a Siemens diffractometer (D500). A Philips scanning electron microscope (SEM: ES 30 kW) was used to determine the size and shape of the nanoparticles.

### MTT assay

In vitro MTT assay was performed on A549 cell line for the three groups in triplicate including the blank, the oleic acid coated Nd<sup>3+</sup>:Gd<sub>2</sub>O<sub>3</sub> and bare nanoparticles according to the Zeini et al. study [23].

### MRI experiments

Similar concentrations of the oleic acid coated Gd<sub>2</sub>O<sub>3</sub> and Nd<sup>3+</sup>:Gd<sub>2</sub>O<sub>3</sub> nanoparticles were prepared and fixed in agarose gel to provide uniform dispersion. Both series of the samples were put in the 3 mL Eppendorf plastic tubes to prevent any imaging artifacts. The Eppendorf tubes were placed in a Perspex water

filled phantom. The T1 and T2 weighted images of the nanoparticles were prepared with a 1.5 Tesla MRI system (Philips, Ingenia).

The spin echo T1 weighted MR images were acquired using the variable TRs (100 to 2500 ms) and a fix TE (8 ms), flip angle = 90 degree, field of view (FOV) = 190 mm<sup>2</sup>, slice thickness = 6 mm<sup>2</sup> and acquisition pixel size = 0.95 × 0.75 mm<sup>2</sup>. For preparing the T2 weighted MR images, a multi spin echo sequence was utilized with a fix TR (4000 msec) and 16 alternate TEs (16 to 256 ms). Other imaging parameters were similar to the T1 weighted images.

Signal intensity of each image was measured by DICOM software of the MRI machine. Plotting the curves of the T1 and T2 relaxation times was done by MATLAB software. The relaxivity graphs which show changes of the 1/T1 and 1/T2 versus Gd<sup>3+</sup> concentrations of the oleic acid coated Gd<sub>2</sub>O<sub>3</sub> and Nd<sup>3+</sup>:Gd<sub>2</sub>O<sub>3</sub> nanoparticles were plotted by excel software.

## Results

### Characterization tests and MTT assay

Figure 1 shows the XRD pattern of the oleic acid coated Nd<sup>3+</sup>:Gd<sub>2</sub>O<sub>3</sub> nanoparticles. The

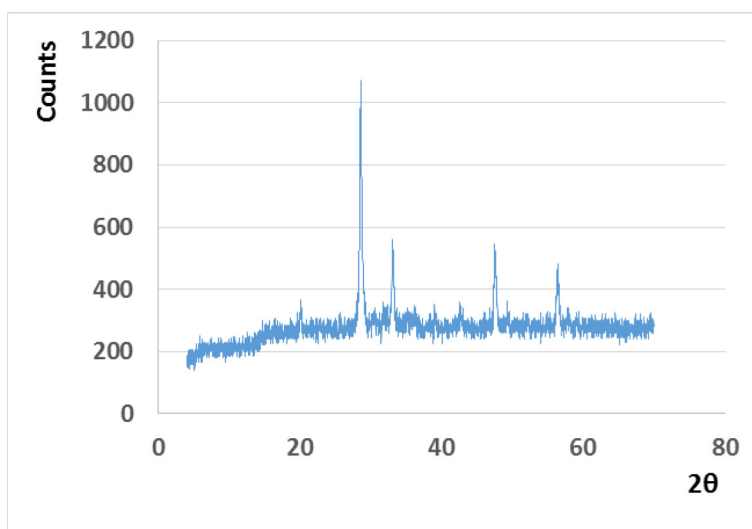


**Figure 1:** X-ray diffraction (XRD) pattern of the oleic acid coated Nd<sup>3+</sup>:Gd<sub>2</sub>O<sub>3</sub> nanoparticles.

Gd<sub>2</sub>O<sub>3</sub> nanoparticles peaks are seen in the figure while there is no peak related to neodymium.

The SEM image of the oleic acid coated Nd<sup>3+</sup>:Gd<sub>2</sub>O<sub>3</sub> nanoparticles is seen in Figure 2. According to the figure, the spherical-like nanoparticles were uniform in the shape and the average size of them was 40 nm.

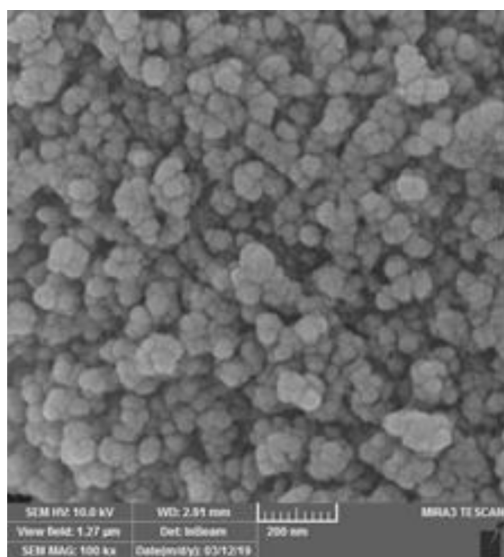


**Figure 2:** Scanning electron microscope (SEM) image of the oleic acid coated Nd<sup>3+</sup>:Gd<sub>2</sub>O<sub>3</sub> nanoparticles.

The cell toxicity of the Nd<sup>3+</sup>:Gd<sub>2</sub>O<sub>3</sub> nanoparticles with and without oleic acid coating is illustrated in Figure 3. Reduction of A549 cells viability with increasing of the concentrations of both nanoparticles is seen in the figure. The coated Nd<sup>3+</sup>:Gd<sub>2</sub>O<sub>3</sub> (light brown columns) and the bare nanoparticles (blue columns) showed a cell viability more than 80% up to concentrations of 0.18 and 0.10 mM, respectively.

### MRI

The T1 and T2 weighted images of the various concentrations of the oleic acid coated Gd<sub>2</sub>O<sub>3</sub> and Nd<sup>3+</sup>:Gd<sub>2</sub>O<sub>3</sub> nanoparticles are shown in the insets of Figures 4A and B, respectively. In the T1 weighted images (inset of Figure 4A), the signal intensity of the Gd<sub>2</sub>O<sub>3</sub> nanoparticles was much higher than that of Nd<sup>3+</sup>:Gd<sub>2</sub>O<sub>3</sub> at similar concentrations. Inset of Figure 4B illustrates the concentration dependent signal intensity reduction for both the oleic acid coated Gd<sub>2</sub>O<sub>3</sub> and Nd<sup>3+</sup>:Gd<sub>2</sub>O<sub>3</sub> nanoparticles with a higher effect on the neodymium doped nanoparticles.

The r1 relaxivity of the oleic acid coated Gd<sub>2</sub>O<sub>3</sub> and Nd<sup>3+</sup>:Gd<sub>2</sub>O<sub>3</sub> nanoparticles were calculated as 24.051 and 2.974 mM<sup>-1</sup>s<sup>-1</sup>, re-

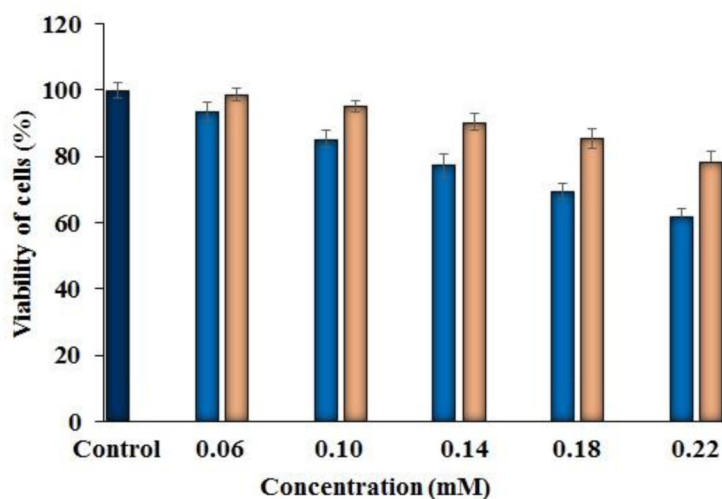


**Figure 3:** 3-(4,5-dimethylthiazol-2-yl)-2,5-diphenyltetrazolium bromide (MTT) assay results for the oleic acid coated Nd<sup>3+</sup>:Gd<sub>2</sub>O<sub>3</sub> nanoparticles (light brown columns) and the bare nanoparticles (blue columns).

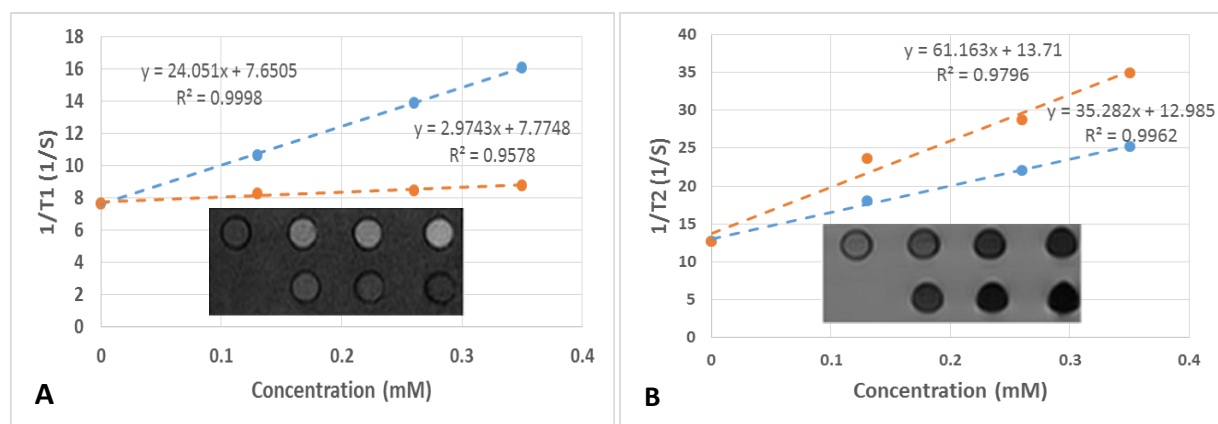


**Figure 4:** A) r1 and B) r2 relaxivity graphs of the oleic acid coated Gd<sub>2</sub>O<sub>3</sub> and Nd<sup>3+</sup>:Gd<sub>2</sub>O<sub>3</sub> nanoparticles. Inset of Figure A and B show the T1 and T2 weighted images of the nanoparticles, respectively. In each inset, the first row demonstrates the zero concentration (at left) and from the low to the high concentrations of the coated Gd<sub>2</sub>O<sub>3</sub> nanoparticles. The second row is related to the same concentrations of the coated Nd<sup>3+</sup>:Gd<sub>2</sub>O<sub>3</sub> nanoparticles.

spectively (Figure 4A). On the other hand, the r2 relaxivity of the coated Nd<sup>3+</sup>:Gd<sub>2</sub>O<sub>3</sub> nanoparticles was calculated as 61.163 mM<sup>-1</sup>s<sup>-1</sup> while it was 35.282 mM<sup>-1</sup>s<sup>-1</sup> for the Gd<sub>2</sub>O<sub>3</sub> nanoparticles (Figure 4B).

## Discussion

### Characterization tests

According to Figure 1 which shows the XRD pattern of the Nd<sup>3+</sup>:Gd<sub>2</sub>O<sub>3</sub> nanoparticles, the main characteristic peaks were matched with the Gd<sub>2</sub>O<sub>3</sub> in cubic phase (JCPDS: 12-0797) with space group Ia3. The XRD peaks were related only to the Gd<sub>2</sub>O<sub>3</sub> nanoparticles and there were no peaks corresponding to neodymium. The finding indicates successful doping of Nd<sup>3+</sup> into the Gd<sub>2</sub>O<sub>3</sub> nanoparticles.

As it is seen in Figure 3, the oleic acid coated Nd<sup>3+</sup>:Gd<sub>2</sub>O<sub>3</sub> nanoparticles showed cytocompatibility at the higher concentrations compared to the bare nanoparticles. The cell viability for the coated nanoparticles was slightly lower than 80% only at the highest concentration (0.22 mM). On the other hand, the bare Nd<sup>3+</sup>:Gd<sub>2</sub>O<sub>3</sub> nanoparticles were cytocompat-

ible only at the lower concentrations (up to 0.10 mM), showing significant effect of the oleic acid coating on the cytocompatibility of the nanoparticles.

### MRI

The higher signal intensity of the Gd<sub>2</sub>O<sub>3</sub> nanoparticles compared to the Nd<sup>3+</sup>:Gd<sub>2</sub>O<sub>3</sub> particles at similar concentrations (inset of Figure 4A) indicates stronger effect of the Gd<sub>2</sub>O<sub>3</sub> nanoparticles on the T1 shortening of the water protons.

An appropriate Gd-based T1 contrast agent enhances the signal intensity and contrast in the T1 weighted MR images proportional to the gadolinium ions concentration. Therefore, the samples with the higher concentrations of gadolinium ions show the higher signal intensity. In the oleic acid coated Nd<sup>3+</sup>:Gd<sub>2</sub>O<sub>3</sub> nanoparticles, some of the gadolinium ions are replaced with Nd<sup>3+</sup>, leading to the changes in the magnetic domains which affect the T1 relaxation time, and consequently, r1 relaxivity. The value of r1 relaxivity is an important factor to determine the efficacy of Gd-based nanoparticles. Based on the r1 re-

laxivity graphs of the oleic acid coated  $Gd_2O_3$  and  $Nd^{3+}:Gd_2O_3$  nanoparticles, the  $r_1$  values were calculated as 24.051 and 2.974  $mM^{-1}s^{-1}$ , respectively (Figure 4A). Consequently, the  $r_1$  value of the  $Gd_2O_3$  nanoparticles was obtained about 8 times higher compared to the  $Nd^{3+}:Gd_2O_3$  nanoparticles.

Despite oleic acid coating of the  $Gd_2O_3$  nanoparticles which is a hydrophobic coating material, the  $r_1$  relaxivity of the nanoparticles in this study is also higher than those of the nanostructures in the other studies such as the ultrasmall  $Gd_2O_3$  nanoparticles with coating of polyethylene glycol diacid (PEGD)-250 and PEGD-600 [24], and the polyethylenimine (PEI) coated ultrasmall  $Gd_2O_3$  nanoparticles (PEI-1300) [25]. Although the physicochemical properties of the  $Gd_2O_3$  nanoparticles are different among the studies, the main reason for the higher  $r_1$  relaxivity of the  $Gd_2O_3$  nanoparticles in this work is their hollow sphere structure. Preparation of the nanoparticles in the present study was carried out by polymer pyrolysis method, leading to production of the hollow sphere  $Gd_2O_3$  nanoparticles. This situation provides a high access of the gadolinium ions to the water protons, and therefore, a high T1 shortening and  $r_1$  relaxivity is resulted.

The oleic acid coated  $Nd^{3+}:Gd_2O_3$  nanoparticles showed the higher T2 effect and image darkness in the T2 weighted images compared to the  $Gd_2O_3$  nanoparticles (inset of Figure 4B). As it is seen in Figure 4B, the  $r_2$  relaxivity of the coated  $Nd^{3+}:Gd_2O_3$  nanoparticles ( $61.163\ mM^{-1}s^{-1}$ ) was about 1.7 times higher than that of the  $Gd_2O_3$  nanoparticles ( $35.282\ mM^{-1}s^{-1}$ ). This finding implies a dominant T2 shortening effect in the  $Nd^{3+}:Gd_2O_3$  nanoparticles due to the doping of the  $Nd^{3+}$  into the nanoparticles which accelerates the spin-spin interactions.

The  $r_2/r_1$  ratio for the  $Gd_2O_3$  and  $Nd^{3+}:Gd_2O_3$  nanoparticles were calculated to be 1.467 and 20.566, respectively. The  $r_2/r_1$  ratio is an indicator to determine whether a magnetic material enhances T1 or T2 contrast of MR im-

ages. Since the value of  $r_2/r_1$  for the  $Gd_2O_3$  nanoparticles is close to unity, the material is considered as a T1 contrast agent. On the other hand, the  $Nd^{3+}:Gd_2O_3$  nanoparticles with a high amount of the  $r_2/r_1$  ratio have potential to enhance T2 contrast of the images.

Comparing the  $r_1$  relaxivity of the oleic acid coated  $Nd^{3+}:Gd_2O_3$  nanoparticles with other lanthanide doped  $Gd_2O_3$  nanoparticles in the similar magnetic field intensity showed the lower  $r_1$  for the  $Nd^{3+}$  doped nanoparticles compared to the terbium doped [13] and the europium doped [26] nanoparticles. It can be due to the different effect of  $Nd^{3+}$  doping on the magnetic domains of the  $Gd_2O_3$  nanoparticles compared to terbium and europium. Since the  $r_2$  values of the terbium doped and europium doped  $Gd_2O_3$  nanoparticles were not reported, comparing the  $r_2$  amounts was not possible.

## Conclusion

In the current study, we investigated the effect of  $Nd^{3+}$  doping on  $r_1$  and  $r_2$  relaxivities of the  $Gd_2O_3$  nanoparticles. The oleic acid coated  $Gd_2O_3$  and  $Nd^{3+}:Gd_2O_3$  nanoparticles were prepared. The successful preparation of the nanoparticles and their compatibility with the A549 cells for 24 h incubation were confirmed by XRD and MTT assay results, respectively. The average size of the spherical-like shape nanoparticles was 40 nm. A considerable drop in the  $r_1$  relaxivity and an improvement in the  $r_2$  relaxivity were observed for the oleic acid coated  $Nd^{3+}:Gd_2O_3$  nanoparticles compared to the  $Gd_2O_3$  particles. The findings revealed that  $Nd^{3+}$  doping into the  $Gd_2O_3$  nanoparticles leads to the changes in the MRI properties of the  $Gd_2O_3$  nanoparticles.

## Acknowledgment

This study was derived from MSc thesis and it was financially supported by Medical Radiation Sciences Research Team of Tabriz University of Medical Sciences (Grant No: 1397.144). The MR imaging was performed at Urmia Emam Reza hospital affiliated with

Iranian Social Security Organization.

## Conflict of Interest

None

## References

1. Coran A, Ortolan P, Attar S, Alberioli E, Perissinotto E, Tosi AL, et al. Magnetic resonance imaging assessment of lipomatous soft-tissue tumors. *In Vivo*. 2017;**31**(3):387-95. doi: 10.21873/invivo.11071. PubMed PMID: 28438867. PubMed PMID: PMC5461449.
2. Cao Y, Xu L, Kuang Y, Xiong D, Pei R. Gadolinium-based nanoscale MRI contrast agents for tumor imaging. *J Mater Chem B*. 2017;**5**(19):3431-61. doi: 10.1039/c7tb00382j. PubMed PMID: 32264282.
3. Boehm-Sturm P, Haeckel A, Hauptmann R, Mueller S, Kuhl CK, Schellenberger EA. Low molecular-weight iron chelates may be an alternative to gadolinium-based contrast agents for T1-weighted contrast-enhanced MR imaging. *Radiology*. 2017;**286**(2):537-46. doi: 10.1148/radiol.2017170116. PubMed PMID: 28880786.
4. Mishra SK, Kannan S. Doxorubicin-conjugated bimetallic silver-gadolinium nanoalloy for multimodal MRI-CT-optical imaging and pH-responsive drug release. *ACS Biomater Sci Eng*. 2017;**3**:3607-19. doi: 10.1021/acsbiomaterials.7b00498.
5. Ghaderi S, Divband B, Gharehaghaji N. Magnetic resonance imaging property of doxorubicin-loaded gadolinium/13X zeolite/folic acid nanocomposite. *J Biomed Phys Eng*. 2020;**10**(1):103-10. doi: 10.31661/jbpe.v0i0.1254. PubMed PMID: 32158717. PubMed PMID: PMC7036414.
6. Zhang G, Gao J, Qian J, Zhang L, Zheng K, Zhong K, et al. Hydroxylated mesoporous nanosilica coated by polyethylenimine coupled with gadolinium and folic acid: a tumor-targeted T1 magnetic resonance contrast agent and drug delivery system. *ACS Appl Mater Interfaces*. 2015;**7**(26):14192-200. doi: 10.1021/acscami.5b04294. PubMed PMID: 26084052.
7. Ni D, Bu W, Ehlerding EB, Cai W, Shi J. Engineering of inorganic nanoparticles as magnetic resonance imaging contrast agents. *Chem Soc Rev*. 2017;**46**(23):7438-68. doi: 10.1039/c7cs00316a. PubMed PMID: 29071327. PubMed PMID: PMC5705441.
8. Chowdhury MA. Metal-organic-frameworks for biomedical applications in drug delivery, and as MRI contrast agents. *J Biomed Mater Res A*. 2017;**105**(4):1184-94. doi: 10.1002/jbm.a.35995. PubMed PMID: 28033653.
9. Ahmad MY, Ahmad MW, Cha H, Oh IT, Tegafaw T, Miao X, et al. Cyclic RGD-coated ultrasmall Gd<sub>2</sub>O<sub>3</sub> nanoparticles as tumor-targeting positive magnetic resonance imaging contrast agents. *Eur J Inorg Chem*. 2018;**2018**:3070-9. doi: 10.1002/ejic.201800023.
10. Dutta RK, Pandey AC. Fluorescent magnetic gadolinium oxide nanoparticles for biomedical applications. *Nanosci Technol*. 2015;**2**:1-6. doi: 10.15226/2374-8141/2/2/00130.
11. Cho M, Sethi R, Lee SS, Benoit DN, Taheri N, Decuzzi P, et al. Gadolinium oxide nanoplates with high longitudinal relaxivity for magnetic resonance imaging. *Nanoscale*. 2014;**6**:13637-45. doi: 10.1039/c4nr03505d.
12. Ranjan SK, Dey R, Soni AK, Rai VK. Er<sup>3+</sup>-Tm<sup>3+</sup>-Yb<sup>3+</sup>: Gd<sub>2</sub>O<sub>3</sub> upconverting phosphors for sensing and laser-induced heating applications. *IEEE Sens J*. 2016;**16**:8494-500. doi: 10.1109/JSEN.2016.2609139.
13. Chen F, Chen M, Yang C, Liu J, Luo N, Yang G, et al. Terbium-doped gadolinium oxide nanoparticles prepared by laser ablation in liquid for use as a fluorescence and magnetic resonance imaging dual-modal contrast agent. *Phys Chem Chem Phys*. 2015;**17**(2):1189-96. doi: 10.1039/c4cp04380d. PubMed PMID: 25418675.
14. Liu J, Tian X, Luo N, Yang C, Xiao J, Shao Y, et al. Sub-10 nm monoclinic Gd<sub>2</sub>O<sub>3</sub>: Eu<sup>3+</sup> nanoparticles as dual-modal nanoprobe for magnetic resonance and fluorescence imaging. *Langmuir*. 2014;**30**:13005-13. doi: 10.1021/la503228v.
15. Deng H, Chen F, Yang C, Chen M, Li L, Chen D. Effect of Eu doping concentration on fluorescence and magnetic resonance imaging properties of Gd<sub>2</sub>O<sub>3</sub>: Eu<sup>3+</sup> nanoparticles used as dual-modal contrast agent. *Nanotechnology*. 2018;**29**:415601. doi: 10.1088/1361-6528/aad347.
16. Shi HZ, Li L, Zhang LY, Wang TT, Wang CG, Su ZM. Facile fabrication of hollow mesoporous Eu<sup>3+</sup>-doped Gd<sub>2</sub>O<sub>3</sub> nanoparticles for dual-modal imaging and drug delivery. *Dyes Pigments*. 2015;**123**:8-15. doi: 10.1016/j.dyepig.2015.07.015.
17. Lu YR, Gou MY, Zhang LY, Li L, Wang TT, Wang CG, et al. Facile one-pot synthesis of hollow mesoporous fluorescent Gd<sub>2</sub>O<sub>3</sub>: Eu/calcium phosphate nanospheres for simultaneous dual-modal imaging and pH-responsive drug delivery. *Dyes Pigments*. 2017;**147**:514-22. doi: 10.1016/j.dyepig.2017.08.043.
18. Kuo T, Lai W, Li C, Wun Y, Chang H, Chen J,

- et al. AS1411 aptamer-conjugated  $Gd_2O_3$ : Eu nanoparticles for target-specific computed tomography/magnetic resonance/fluorescence molecular imaging. *Nano Res.* 2014;**7**:658-69. doi: 10.1007/s12274-014-0420-4.
19. Li H, Song S, Wang W, Chen K. In vitro photodynamic therapy based on magnetic-luminescent  $Gd_2O_3$ : Yb, Er nanoparticles with bright three-photon up-conversion fluorescence under near-infrared light. *Dalton Trans.* 2015;**44**:16081-90. doi: 10.1039/c5dt01015b.
  20. Liu J, Huang L, Tian X, Chen X, Shao Y, Xie F, et al. Magnetic and fluorescent  $Gd_2O_3$ : Yb<sup>3+</sup>/Ln<sup>3+</sup> nanoparticles for simultaneous upconversion luminescence/MR dual modal imaging and NIR-induced photodynamic therapy. *Int J Nanomedicine.* 2017;**12**:1-14. doi: 10.2147/IJN.S118938. PubMed PMID: 28031709. PubMed PMCID: PMC5179219.
  21. Boopathi G, Raj SG, Kumar GR, Mohan R. Structural and optical properties of Nd<sup>3+</sup> doped gadolinium oxide 1D nanorods. *AIP Conf Proc.* 2014;**1591**:44-5. doi: 10.1063/1.4872483.
  22. Khatamian M, Khandar AA, Divband B, Haghghi M, Ebrahimiasl S. Heterogeneous photocatalytic degradation of 4-nitrophenol in aqueous suspension by Ln (La<sup>3+</sup>,Nd<sup>3+</sup>,Sm<sup>3+</sup>) doped ZnO nanoparticles. *J Mol Catal A Chem.* 2012;**365**:120-7. doi: 10.1016/j.molcata.2012.08.018.
  23. Zeini M, Divband B, Khezerloo D, Gharehaghaji N. Biointerface Research in Applied Chemistry. *Bio-interface Res Appl Chem.* 2019;**9**(4):4101-6. doi: 10.33263/BRIAC94.101106.
  24. Kim CR, Baeck JS, Chang Y, Bae JE, Chae KS, Lee GH. Ligand-size dependent water proton relaxivities in ultrasmall gadolinium oxide nanoparticles and in vivo T1 MR images in a 1.5 T MR field. *Phys Chem Chem Phys.* 2014;**16**:19866-73. doi: 10.1039/c4cp01946f.
  25. Tegafaw T, Xu W, Lee SH, Chae KS, Cha H, Chang Y, et al. Ligand-size and ligand-chain hydrophilicity effects on the relaxometric properties of ultrasmall  $Gd_2O_3$  nanoparticles. *AIP Adv.* 2016;**6**:065114. doi: 10.1063/1.4954182.
  26. Luo N, Yang C, Tian X, Xiao J, Liu J, Chen F, et al. A general top-down approach to synthesize rare earth doped-  $Gd_2O_3$  nanocrystals as dualmodal contrast agents. *J Mater Chem B.* 2014;**2**:5891-7. doi: 10.1039/C4TB00695J.